Int. J. Heat Mass Transfer. Vol. 36, No. 14, pp. 3633–3645, 1993
Printed in Great Britain

0017–9310/93 $6.00 + 0.00

Radiant and convective heat transfer for flow of a radiation gas in a heated/cooled tube with a grey wall

J. STASIEK† and M. W. COLLINS‡

† Technical University of Gdansk, Gdansk, Poland
‡ Thermo-Fluids Engineering Research Centre, City University, London, U.K.

(*Received* 23 *December* 1991)

Abstract—An analytical investigation is presented of the influence of radiative heat transfer on the complex heat exchange problem involving flow of an optically active (radiating) gas inside a tube of diffuse grey properties. The method used is based on Hottel's formulation of zone division, and involves the transformation-zone approach, where radiation gas emission is replaced with an equivalent surface emission. Separable-kernel and surface transformation techniques give a set of non-linear differential equations treated by the Runge–Kutta method with Hamming modification. The solutions are governed by several independent parameters such as the wall and radiation gas emissivities, inlet and exit gas temperatures, length–diameter ratio of the tube, uniform and non-uniform heat flux and variable convective heat transfer coefficient at the inner surface. The results apply both to heating and cooling situations.

INTRODUCTION

THE THERMAL design and analysis of energy conversion systems and devices such as furnaces, combustion chambers, combustors, fluidized beds, and open cycle coal- and natural-gas-fires MHD must often take account of the effects of thermal radiation. Radiation is also a significant mode of heat transfer in many high temperature technological areas such as heating and annealing furnaces, thermal control of spacecraft, nuclear reactor safety and fire spread. In some instances, the radiation will impose an additional heat load on a part which is to be kept cool, and hence this exchange must be estimated when the cooling requirements are computed. In other cases, the radiation will cause a region operating at a high temperature to have it reduced.

Heat transfer by forced convection to a gas flowing in a tube has received detailed study in the literature, but little consideration has been given to the added effects caused when thermal radiation (in participating media) is also present. The situation considered here is the heat exchange in a circular tube with a uniform or non-uniform heat flux supplied along the wall, and there is a constant or variable convective heat transfer coefficient at the inner surface.

The purpose of this paper is to examine the interaction of radiative and convective transfers for flow of a radiation gas in a circular tube. The present paper also provides the additional analysis necessary to extend refs. [1–3] to include a radiative contribution of a radiation gas. The proposed method which includes the influence of gas emission is based on the zone division approach first formulated by Hottel [4, 5] and developed by Siegel and Perlmutter [1, 2, 6]. In this, the non-isothermal gas and surface are divided into infinitely small isothermal elements. Also, it involves the transformation-zone technique, where the emission of the gas body is replaced with an equivalent surface emission [1, 7–10].

Previously, the analysis presented here has been applied to heated tubes only, [8, 9], whereas, in fact, it is equally valid for cooled tubes. This is made explicit in the final derived equation where the upper and lower signs refer to heated and cooled conditions, respectively. Also, the analysis is a development of that presented by Siegel and Perlmutter [2] and Perlmutter and Siegel [1]. We have deliberately used the same notation and derivation to enable the reader to appreciate the additional features of this work.

ANALYSIS

The system to be analysed is shown schematically in Fig. 1 (the tube system treated here is similar to that studied by Siegel and Perlmutter [1, 2]). A radiative gas at a specified inlet temperature $T_{g,i}$ flows into the tube and is heated to an average exit temperature $T_{g,e}$. A uniform or non-uniform heat flux $q(X)$ is supplied to the tube wall by external means, and the outside surface of the tube is assumed to be insulated. Each end of the tube is exposed to an outside environment or reservoir at specified temperatures, $T_{r,i}$ and $T_{r,e}$ at the inlet and exit of the tubes respectively. The inside of the tube wall is a diffuse grey surface with an emissivity ε. The Planck mean volume absorption coefficient α is constant and the optical thickness $\kappa \ll 1$. It is assumed that there is no axial conduction in the tube wall or in the radiation gas and that the convection heat transfer coefficient $h(X)$ is non-uniform throughout the tube.

NOMENCLATURE

A	area of relation of absorptivity and apparent emissivity of radiation gas
a_p	apparent absorptivity of radiation gas surface
C	dimensionless constant of parabolic distribution from equation (23)
c	constant of parabolic distribution
c_p	specific heat of fluid
D	tube diameter
E	substitute emissivity factor
e	emissive power, emissivity per unit area
F	geometric configuration factor for radiation from an element on the tube wall to the circular opening at the end of the tube or the apparent surface of the radiation gas body
$H(x)$	dimensionless length-dependent heat-transfer coefficient
H, H_1, H_2	dimensionless constants from equation (22)
$h(x)$	convective length-dependent heat-transfer coefficient
h, h_1, h_2	constants in equation (3)
I	energy of flowing gas
K	geometric configuration factor between elements on the inside of the tube wall
k	dimensionless radiation gas absorption coefficient, αD
L	length of tube
l	dimensionless length, L/D
Q	energy rate, energy per unit time
$q(x)$	heat added per unit area at tube wall (length-dependent)
q	constant of parabolic distribution, energy flux
q_i^*	total incoming radiation per unit area to a surface element
q_o	total outgoing radiation per unit area from a surface element
M	dimensionless constant of parabolic distribution from equation (23)
m	constant of parabolic distribution
N	radiation heat-transfer coefficient
R	dimensionless radiation heat-transfer coefficient
$S(x)$	length-dependent Stanton number
S, S_1, S_2	dimensionless constants from equation (14)
T	temperature
t	dimensionless temperature
u_m	mean radiation gas velocity
X	axial length coordinate measured from tube entrance
x	dimensionless coordinate, X/D
Y	dummy integration variable.

Greek symbols

α	absorption coefficient
ξ	dimensionless variable, Y/D
ε	emissivity of surface
ε_p, $d(\varepsilon_{p,i})$	apparent emissivity of radiation gas body surface
ε_e	effective emissivity factor
ρ	density of radiation gas
σ	Stefan–Boltzmann constant
τ	transmissivity.

Subscripts

b	blackbody
e	exit end of tube
g	gas
i	inlet end of tube (except in symbol q_i^* and $d(\varepsilon_{p,i})$)
p	apparent surface of radiation gas body
r	reservoir
w	inside surface of tube wall.

Energy balance

The analytical relation between temperatures and heat fluxes can be obtained from an energy balance for the elementary surface dA_i and gas volume dV_i. According to the net radiation method of Poljak [6], and other workers [2, 3] the energy balance for an elementary surface dAx a distance X from the tube inlet equals

$$q_i^*(X)+q(X) = q_o(X)+h(X)[T_w(X)-T_g(X)]. \quad (1)$$

The terms on the left are, respectively, the total incoming radiation and the flux due to wall heating. On the right-hand side, the respective terms are the radiative heat flux leaving the surface element and the heat flowing by convection from the wall to gas. (T_w-T_g) is the local difference between the wall temperature and bulk gas temperature. The imposed heat flux $q(X)$ and convective heat transfer coefficient $h(X)$ are assumed to be dependent on axial position

$$q(X) = q+mX+cX^2 \quad (2)$$

and

$$h(X) = h+h_1X+h_2X^2 \quad (3)$$

that is, parabolic distributions.

The radiation terms are now considered in detail. $q_o(X)$ is composed both of direct emission $\varepsilon\sigma T_w^4$, and reflected radiation which is $(1-\varepsilon)$ times the total

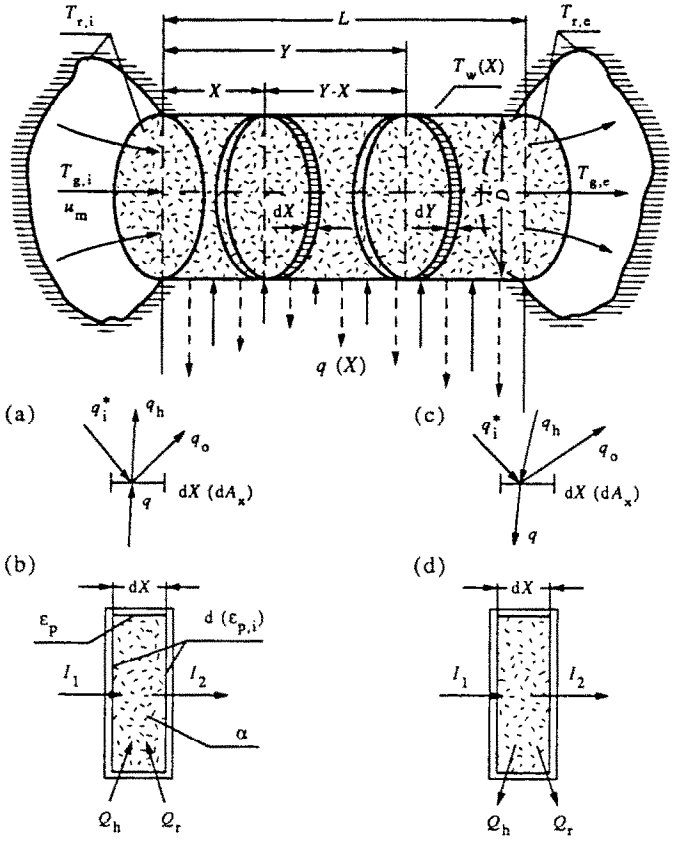

FIG. 1. Circular tube geometry. (a) Energy quantities incident upon and leaving infinitesimal surface dA_x and (b) energy quantities for gaseous volume element dV_x for heated tube and (c) and (d) for cooled tube, respectively.

incoming radiation [2, 6]

$$q_o(X) = \varepsilon\sigma T_w^4 + (1-\varepsilon)q_i^*(X). \tag{4}$$

The total incoming radiative heat flux $q_i^*(X)$ is composed of three types of terms, the radiation coming from the reservoirs at the ends of the tube, the radiation from the other elements on the internal tube surface, and the radiation arriving from elementary gas bodies in the form of cylindrical slices (Fig. 1) [3, 8]. These quantities can be written as

$$\begin{aligned} q_i^*(X) = {} & \sigma T_{r,i}^4 \tau(X)F(X) + \sigma T_{r,e}^4 \tau(L-X)F(L-X) \\ & + \int_0^X q_o(Y)\tau(X-Y)K(X-Y)\,dY \\ & + \int_X^L q_o(Y)\tau(Y-X)K(Y-X)\,dY \\ & + \int_0^X e_{g,b}\,d(\varepsilon_{p,Y})\tau(X-Y)F(X-Y) \\ & + \int_X^L e_{g,b}\,d(\varepsilon_{p,Y})\tau(Y-X)F(Y-X). \end{aligned} \tag{5}$$

In equation (5) the functions $F(Z)$ and $K(Z)$ are the typical geometrical configuration factors which occur in the system under consideration and $\tau(Z)$ is the gas transmissivity of thickness Z [1, 2]. The quantity $d(\varepsilon_{p,Y})$ is the apparent emissivity of the real surface of the gas body. This apparent emissivity is given by [3, 8]

$$d(\varepsilon_{p,i}) = 1.5\alpha D\,dX = 1.5k\,dX. \tag{6}$$

By substituting equation (5) into equation (1) and equation (4) into equation (1), one obtains two relations which include q_o, T_w and T_g as a function of the dimensionless independent variable x [3, 8, 10]

$$\begin{aligned} & q_o(x) + h(x)[T_w(x) - T_g(x)] = q(x) \\ & \quad + \sigma T_{r,i}^4 \tau(x)F(x) + \sigma T_{r,e}^4 \tau(l-x)F(l-x) \\ & \quad + \int_0^x q_o(\zeta)\tau(x-\zeta)K(x-\zeta)\,d\zeta \\ & \quad + \int_x^l q_o(\zeta)\tau(\zeta-x)K(\zeta-x)\,d\zeta \\ & \quad + \int_0^x e_{g,b}\,d(\varepsilon_{p,\zeta})\tau(x-\zeta)F(x-\zeta) \\ & \quad + \int_x^l e_{g,b}\,d(\varepsilon_{p,\zeta})\tau(\zeta-x)F(\zeta-x) \end{aligned} \tag{7}$$

and

$$q_o(x) = \frac{1-\varepsilon}{\varepsilon}\{h(x)[T_w(x)-T_g(x)]-q(x)\}+\sigma T_w^4(x). \tag{8}$$

In order to solve the set of equations (7) and (8), an additional heat balance is written for the flowing radiation gas. Since the gas is non-transparent to radiation, heat is transferred to the wall both by convection Q_h and radiation Q_r. For a cylindrical volume element of length dX and diameter D, the heat transferred is [3, 7, 8, 11]

$$Q_h = h(X)[T_w(X)-T_g(X)]\pi D\,dX \tag{9}$$

and

$$Q_r = \frac{\sigma\varepsilon_p}{a_p\left[\frac{1}{\varepsilon}+\frac{1}{a_p}-1\right]}[AT_w^4(X)-T_g^4(X)]\pi D\,dX \tag{10}$$

where

$$A = \frac{a_p}{\varepsilon_p};\ \varepsilon_p = \frac{\alpha D}{4} = \frac{k}{4}. \tag{11}$$

ε_p is the apparent emissivity of an incremental length of grey gas which is infinitely small. This contrasts with $d(\varepsilon_{p,l})$, which is the apparent emissivity of the real gas body surface, given by equation (6).

Equation (10) is the same as equation (8; 10) of Hottel and Sarofim (pp. 301–302 of ref. [11]). However, that equation holds for a grey gas surrounded by a single source–sink surface, where both gas and surface are at uniform temperature. This will lead to an error where the temperatures vary, and, in fact, we only use the equation on a differential-length basis. However, the overall energy balance (Δb[%] in Tables 1–8) includes the effect of all considerations such as the above, and may be regarded as quantitatively satisfactory.

The quantity (Q_h+Q_r) is equal to the net heat removed from the volume element by the flowing radiation gas which is

$$I_1 - I_2 = \Delta I = -u_m\frac{\pi D^2}{4}\rho c_p\frac{dT_g(X)}{d(X)}dX. \tag{12}$$

The mean fluid velocity u_m is assumed constant so that kinetic energy changes of the gas are neglected. These three quantities are equated and the result is rearranged into the form [7, 10]

$$\frac{dT_g(x)}{dx} = [S+S_1x+S_2x^2][T_w(x)-T_g(x)] + N[AT_w^4(x)-T_g^4(x)] \tag{13}$$

where

$$S = \frac{4h}{u_m\rho c_p};\quad S_1 = \frac{4h_1D}{u_m\rho c_p};\quad S_2 = \frac{4h_2D^2}{u_m\rho c_p} \tag{14}$$

$$N = \frac{4\sigma\varepsilon_c}{u_m\rho c_p};\quad \varepsilon_c = \frac{\varepsilon_p}{a_p\left[\frac{1}{\varepsilon}+\frac{1}{a_p}-1\right]}. \tag{15}$$

Equation (13) is the third, necessary relation between q_o, T_w and T_g. As two of them, T_w and T_g, describe the physical aspect of the phenomenon, the following transformations are carried out according to their elimination [1, 2].

Transformation to a differential equation

According to the method presented in refs. [1, 2], the integral in equation (8) can be reduced to a differential equation by the use of exponential approximations for the geometric kernel K, configuration factor F and transmissivity T. As shown in refs. [1–3], the functions K, F, τ could be represented quite well by

$$K(x) \cong e^{-2x} \tag{16}$$

$$F(x) \cong \tfrac{1}{2}e^{-2x} \tag{17}$$

$$\tau(x) = e^{-kx}. \tag{18}$$

By substituting (according to refs. [1–3]) the representation given by equations (16)–(18) and by double differentiation of equations (7) and (8) with respect to x, and also by single differentiation of equation (13), one obtains the following set of nonlinear, dimensionless differential equations:

$$\frac{d^2t_w}{dx^2}\left[\frac{H+H_1x+H_2x^2}{\varepsilon}+4t_w^3\right]+12t_w^2\left(\frac{dt_w}{dx}\right)^2 - \left\{\frac{H+H_1x+H_2x^2}{\varepsilon}(S+S_1x+S_2x^2+4RAt_w^3) - \frac{2(H_1+H_2x)}{\varepsilon}\right\}\frac{dt_w}{dx} = \mp 4E$$

$$\mp 4MEx \mp 4CEx^2 \pm \frac{2C}{\varepsilon} + (t_w-t_g)\left\{4E(H+H_1x+H_2x^2) - \frac{2H_2}{\varepsilon}+\frac{2(H_1+H_2x)}{\varepsilon}[S+S_1x+S_2x^2] + \frac{(H+H_1x+H_2x^2)}{\varepsilon}[S_1+S_2x] - \frac{1}{\varepsilon}(H+H_1x+H_2x^2)(S+S_1x+S_2x^2) \times (S+S_1x+S_2x^2+4Rt_g^3)\right\} + t_w^4\left\{k(2+k)+\frac{2(H_1+H_2x)}{\varepsilon}RA - \frac{1}{\varepsilon}(H+H_1x+H_2x^2)(S+S_1x+S_2x^2+4Rt_g^3)RA\right\}$$

$$-t_g^4\left\{2(2+k)\varepsilon_{p,s}-\frac{1}{\varepsilon}(H+H_1x+H_2x^2)\right.$$
$$\left.\times(S+S_1x+S_2x^2+4Rt_g^3)R+\frac{2(H_1+H_2x)}{\varepsilon}R\right\} \quad (19)$$

and

$$\frac{dt_g}{dx}=(S+S_1x+S_2x^2)(t_w-t_g)+R(At_w^4-t_g^4) \quad (20)$$

where

$$t=T\left(\frac{\sigma}{q}\right)^{1/4};\quad E=\frac{k(2+k)(1-\varepsilon)+(2+k)^2\varepsilon}{4\varepsilon} \quad (21)$$

$$H=\frac{h}{q}\left(\frac{q}{\sigma}\right)^{1/4};\quad H_1=\frac{h_1D}{q}\left(\frac{q}{\sigma}\right)^{1/4};\quad H_2=\frac{h_2D^2}{q}\left(\frac{q}{\sigma}\right)^{1/4} \quad (22)$$

$$R=N\left(\frac{q}{\sigma}\right)^{3/4};\quad M=\frac{mD}{q};\quad C=\frac{cD^2}{q};\quad \varepsilon_{p,s}=0.75k. \quad (23)\dagger$$

The terms involving $t_{r,i}$ and $t_{r,e}$ have thus been eliminated, but they will appear in the boundary conditions. The two differential equations (19) and (20) are solved simultaneously by a numerical procedure, but first the boundary conditions have to be specified.

Boundary conditions

Equation (20) is a first order equation requiring only one boundary condition. This condition is that at the inlet of the tube the gas temperature has a specified value $t_{g,i}$

$$t_g=t_{g,i}\quad\text{at}\quad x=0. \quad (24)$$

Equation (19) is a second order equation and requires two boundary conditions. These are given by the use of the approximations for configuration factors and transmissivity.

At $x=0$ this gives

$$\left.\frac{dt_w}{dx}\right|_{x=0}=\frac{1}{[H+4\varepsilon t_w^3(0)]}$$
$$\times\left\{H\left[S+2+k-\frac{H_1}{H}\right][t_w(0)-t_{g,i}]\right.$$
$$\mp(2+k)\pm M+\varepsilon(2+k)t_w^4(0)-\varepsilon(2+k)t_{r,i}^4$$
$$\left.+HR[At_w^4(0)-t_{g,i}^4]\right\} \quad (25)$$

and for $x=l$

$$\frac{1-\varepsilon}{\varepsilon(2+k)}[1+k+e^{-(2+k)l}]\pm\frac{t_{r,i}^4e^{-(2+k)l}}{2}+1$$
$$=\pm\frac{1}{\varepsilon}[H+H_1l+H_2l^2][t_w(l)-t_g(l)]$$
$$\pm t_w^4(l)\mp\frac{t_{r,e}^4}{2}\mp\varepsilon_{p,s}e^{-(2+k)l}\int_0^l t_g^4$$
$$\times e^{(2+k)x}\,dx\mp e^{-(2+k)l}\int_0^l\left[\frac{1-\varepsilon}{\varepsilon}(H+H_1x+H_2x^2)\right.$$
$$\left.\times(t_w-t_g)+t_w^4\right]e^{(2+k)x}\,dx$$
$$+M\left\{\left[\frac{l}{(2+k)}-\frac{1}{(2+k)^2}\right.\right.$$
$$\left.\left.+\frac{1}{(2+k)^2}e^{-(2+k)l}\right]\frac{1-\varepsilon}{\varepsilon}-\frac{l}{\varepsilon}\right\}$$
$$+C\left\{\left[\frac{l^2}{(2+k)}-\frac{2l}{(2+k)^2}+\frac{2}{(2+k)^3}\right.\right.$$
$$\left.\left.-\frac{2}{(2+k)^3}e^{-(2+k)l}\right]\frac{1-\varepsilon}{\varepsilon}-\frac{l^2}{\varepsilon}\right\}. \quad (26)$$

The procedure which yields boundary conditions (24)–(26) is presented in refs. [1–3]. However, the solution procedure involved assuming $t_w(0)$ and calculating the first derivative with respect to x at the wall. The boundary condition for $x=l$ is used for verification of the overall calculation which comes to an end when the condition is satisfied.

Overall heat balance

In research practice, despite the formal satisfaction of boundary conditions, a numerical solution also requires the overall thermal balance of the system to be correct [1, 2]. According to refs. [1–3, 8], the heat balance takes the dimensionless form

$$l+\frac{Ml^2}{2}+\frac{Cl^3}{3}\pm\frac{H}{S}t_{g,i}\pm\frac{t_{r,i}^4}{2(2+k)}[1-e^{-(2+k)l}]$$
$$\pm\frac{1-\varepsilon}{\varepsilon(2+k)}[1-e^{-(2+k)l}]\pm\frac{t_{r,e}^4}{2(2+k)}[1-e^{-(2+k)l}]$$
$$=\pm\frac{H}{S}t_{g,e}\pm\frac{1}{2}\int_0^l\left[\frac{1-\varepsilon}{\varepsilon}(H+H_1x+H_2x^2)\right.$$
$$\left.\times(t_w-t_g)+t_w^4\right][e^{-(2+k)x}+e^{-(2+k)(l-x)}]\,dx$$
$$\pm\tfrac{1}{2}\varepsilon_{p,s}\int_0^l t_g^4[e^{-(2+k)x}+e^{-(2+k)(l-x)}]\,dx\pm\varphi \quad (27)$$

where

$$\varphi=\frac{1-\varepsilon}{\varepsilon}\left\{-\frac{Ml}{(2+k)}(1-e^{-(2+k)l})\right.$$
$$+C\left[-\frac{l^2}{(2+k)}+\frac{2l}{(2+k)^2}-\frac{4}{(2+k)^3}\right]$$
$$\left.+C\left[e^{-(2+k)l}\left(\frac{l^2}{(2+k)}+\frac{2l}{(2+k)^2}+\frac{4}{(2+k)^3}\right)\right]\right\}. \quad (28)$$

† $\varepsilon_{p,g}$ arises from the identity (from equation (7)) of $d(\varepsilon_{p,\xi})F(\xi-x)=1.5k\,dx F(\xi-x)=1.5k\,dx\,K(\xi-x)/2=0.75k\,dx\,K(\xi-x)=\varepsilon_{p,s}\,dx\,K(\xi-x)$.

From the preceding set of non-linear differential equations, together with the boundary conditions and the overall heat balance, it is necessary first to determine the independent parameters: H; H_1; H_2; S; S_1; S_2; ε; A; k; R; l; $t_{r,i}$; $t_{r,e}$ and $t_{g,i}$. Then it requires an approximation of the value for $t_w(0)$ and the evaluation of dt_w/dx for $x = 0$ from equation (25). This calculation enables a further solution of equations (19) and (20) to be made, a procedure described in detail in refs. [1–3].

NUMERICAL RESULTS

The set of non-linear differential equations (19) and (20) was solved by the Runge–Kutta method with the Hamming modification, use being made of the IBM standard library. The calculations were performed on an IBM PC computer. In refs. [1, 2] the overall problem was treated by various calculations. The inside of the tube wall was assumed to be a black or diffuse grey surface and the gas flowing through the tube was transparent to radiation. The convective heat-transfer coefficient between the tube wall and the gas was assumed constant—for simplicity the heat addition at the tube wall was specified to be uniform. The solutions are governed by seven independent parameters such as the wall emissivity, inlet gas temperature, inlet and exit reservoir temperatures and length–diameter ratio of the tube. Numerical examples are given to show the influence of these parameters and to demonstrate how radiation alters the wall temperature distribution that would exist for convection alone. In this paper, therefore, we concentrate on certain specific results. These illustrate the influence of (i) the radiative properties of the radiation gas and wall, (ii) the non-uniformity of a heat flux imposed at the wall and (iii) the non-uniformity of a convection heat-transfer coefficient on the wall, t_w, and gas, t_g, temperature distribution. All the above relates to heated tubes. As has been stated, the analysis is equally valid for cooled tubes, and results for these are now considered. However, only illustrative examples are given. Also, in Tables 1–8 is an expression of the accuracy of the method Δb[%]. It has already been mentioned that the outlet boundary condition given by equation (26) is a termination criterion. For this, a precision parameter was defined as being the ratio of the difference between the left- and right-hand sides of equation (26) divided by the right-hand side. For this study, the parameter was set at 0.01%. A similar Δb was defined for the overall energy balance, equation (27), the values for the various calculation runs being in Tables 1–8. These values are partly a reflection of the parameter for equation (26), but mainly an expression of the overall accuracy of the method. In future work, we intend to study the relative effects of the contributing factors to the error in question. Further, it would be feasible to compare such considerations with those in other methods, for instance the Monte-Carlo, or heat flux, approaches.

Results for heated short tubes

Numerical calculations have been obtained for a heated short tube having a length–diameter ratio of 5. The values of the parameters were chosen to show the behaviour of the system for various combinations of the independent parameters. For all of the solutions, the inlet and exit reservoir temperatures were set equal, respectively, to the inlet and exit gas temperatures.

Effect of radiation gas absorptivity

The effect of radiation gas absorptivity (in dimensionless form) on the wall and in the radiation gas temperature distribution is shown in Figs. 2(a) and (b) for uniform heat flux and two chosen wall emissivities $\varepsilon = 1.0$ and 0.01. These graphs give new data, then, compared with Siegel and Perlmutter [2] who assumed the gas to be transparent. In Fig. 2(a), curves are given for different values of dimensionless gas absorptivity k between 0.0 and 0.5. When the gas absorptivity is increased, the radiant heat transfer becomes more efficient for $\varepsilon = 1.0$. The temperature distribution along the inner surface of the wall was found to be quite insensitive to this range of the k-parameter for $\varepsilon = 0.01$. For comparison, the curve for pure convection and uniform heat flux is included. The radiation loss to the reservoirs causes the wall temperature to drop near the ends of the tube. As expected, when ε decreases and k increases, a greater portion of the heat is transferred to the radiation gas. This is also shown in Fig. 2(b) where the radiation gas temperature variation approaches that of pure convection as k becomes large and is above the pure convection line (for $k = 0.2$–0.5) if $\varepsilon = 0.01$. Tables 1 and 2 shows the set of dimensionless numbers and physical quantities which were used in the calculation. The initial and final wall and radiation gas temperatures, both calculated numerically, are also presented there. In Fig. 2(c), the solutions in Fig. 2(a) are plotted in terms of the radiation correction factor H/H_{exp}, which was discussed in refs. [1, 2]. The present analysis has predicted the t_w and t_g which would be measured, and a local experimental heat-transfer coefficient can then be defined as [1–3]

$$h_{exp} = \frac{q}{T_w - T_g} \quad \text{or} \quad H_{exp} = \frac{1}{t_w - t_g}. \tag{29}$$

The H_{exp} will result from the combined effects of both radiation and convection. The dimensionless heat-transfer coefficient for convection alone is simply H so that we can form the ratio

$$H/H_{exp} = H(t_w - t_g). \tag{30}$$

The ratio is really a correction factor, and if it is used as a multiplier on the *experimental* results, it will correct for the radiation effect on H_{exp}. The result will be the heat-transfer coefficient for convection alone. For $l = 5$, there are large radiation losses so that the measured heat-transfer coefficient would be much higher than the convection coefficient. In this case the

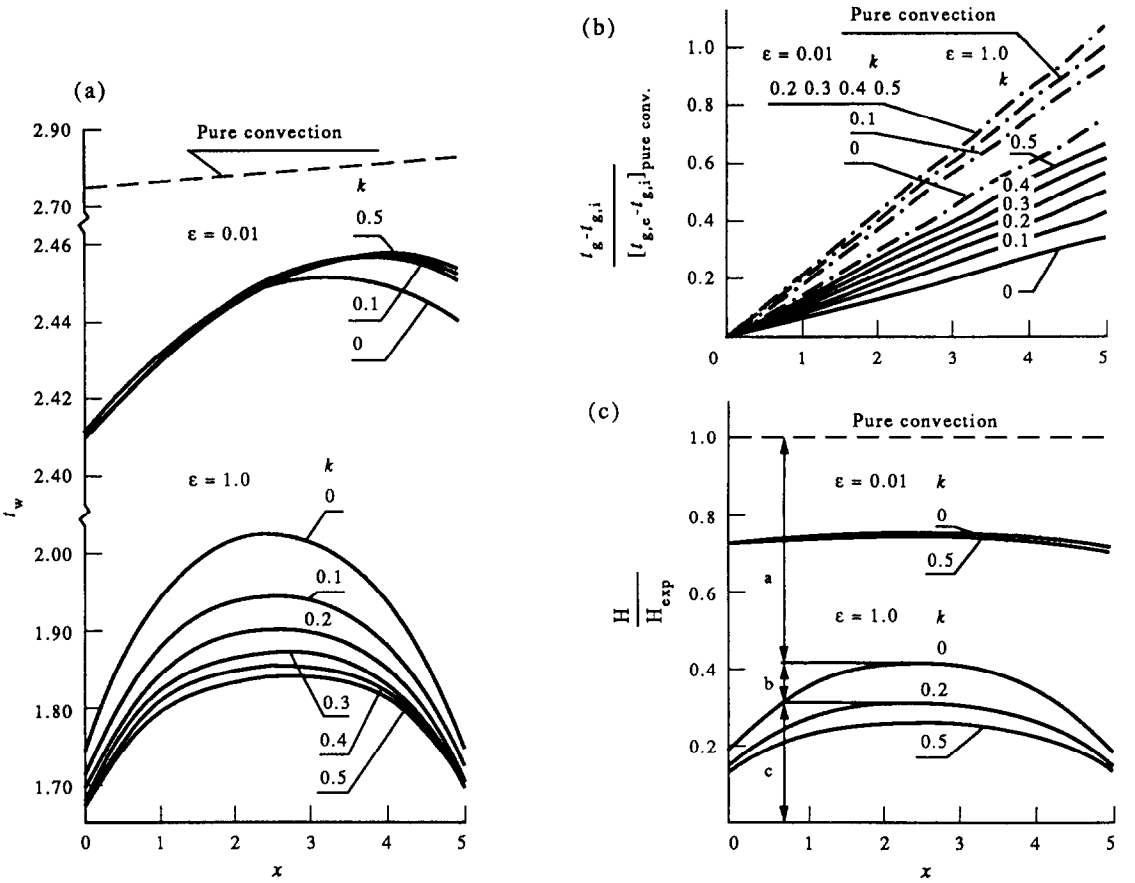

FIG. 2. (a) Effect of dimensionless absorptivity k on temperature distribution in the tube wall. $q(x) = \text{const}$; $\varepsilon = 1.0$ and 0.01. (b) Effect of dimensionless absorptivity k on temperature distribution in the gas. $q(x) = \text{const}$; $\varepsilon = 1.0$ and 0.01. (c) Effect of dimensionless absorptivity k and wall emissivity ε on the ratio of heat transfer for pure convection to that for combined convection and radiation. $q(x) = \text{const}$.

Table 1. Effect on predictions of varying dimensionless absorptivity k, for $\varepsilon = 1.0$ (heated tube)

$\varepsilon = 1.0$ $l = 5$ $H = 0.8$ $S = 0.01$ $t_{r,i} = t_{g,i} = 1.5$ $A = 0.85$						
k	0.0	0.1	0.2	0.3	0.4	0.5
R	0.0	3.12×10^{-4}	6.25×10^{-4}	9.373×10^{-4}	2.25×10^{-4}	1.563×10^{-3}
ε_p	0.0	0.025	0.05	0.075	0.10	0.125
$\varepsilon_{p,s}$	0.0	0.075	0.15	0.225	0.30	0.375
E	1.0	1.1025	1.21	1.3225	1.44	1.5625
$t_w(0) = t_{w,i}$	1.7399	1.7065	1.6894	1.6791	1.6722	1.6674
$t_{w,e} = t_w(l)$	1.7525	1.7237	1.7105	1.7039	1.7006	1.6992
$t_{r,e} = t_{g,e}$	1.5216	1.5266	1.5306	1.5344	1.5380	1.5416
Δb [%]	0.00	0.041	0.066	0.10	0.30	0.52

Table 2. Effect on predictions of varying dimensionless absorptivity k, for $\varepsilon = 0.01$ (heated tube)

$\varepsilon = 0.01$ $l = 5$ $H = 0.8$ $S = 0.01$ $t_{r,i} = t_{g,i} = 1.5$ $A = 0.85$						
k	0.0	0.1	0.2	0.3	0.4	0.5
R	0.0	1.0×10^{-4}	1.4×10^{-4}	1.5×10^{-4}	1.58×10^{-4}	1.62×10^{-4}
ε_p	0.0	0.025	0.05	0.075	0.10	0.125
$\varepsilon_{p,s}$	0.0	0.075	0.15	0.225	0.30	0.375
E	1.0	6.30	12.10	18.40	25.20	32.5
$t_w(0) = t_{w,i}$	2.4093	2.4085	2.4082	2.4080	2.4079	2.4079
$t_{w,e} = t_w(l)$	2.4401	2.4478	2.4510	2.4518	2.4525	2.4529
$t_{r,e} = t_{g,e}$	1.5459	1.5581	1.5629	1.5641	1.5651	1.5656
Δb [%]	0.0	0.57	0.85	0.97	1.09	1.18

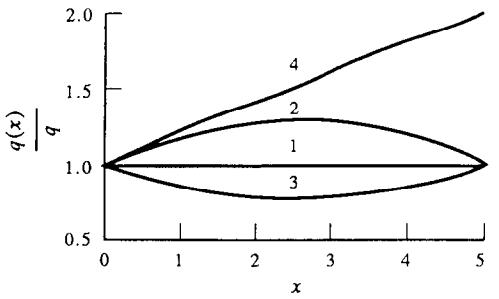

FIG. 3. The heat flux $q(x)/q$ distributions along the tube wall.

set of correction factors is much less than unity. In the central region of the short tube for $\varepsilon = 1.0$ (Fig. 2(c)) about 25% of the heat input is transferred by convection (c) and 75% by radiation (a) and (b) where 15% is the effect of the energy transfer from the radiation gas (b). However, for $l = 5$ and $\varepsilon = 0.01$, radiation accounts for only 25% of the energy transfer and heat exchange from the radiation gas can be neglected. Even for an emissivity as low as 0.01, the correction factor is quite large and the effect of radiation cannot be ignored in comparison with the convection effects [2, 3].

Effect of heat flux

Figure 3 illustrates the heat flux distributions along the tube wall. Numerical calculations show the correct and significant influence of dimensionless heat flux distribution on the temperature distribution t_w and t_g. It is also demonstrated that there is substantial influence of heat flux distribution for a low value of wall emissivity.

The results for different values of heat flux distribution $q(x)/q$ are shown in Figs. 4(a) and (b) for emissivities $\varepsilon = 1$ and 0.01 and dimensionless radiation gas absorptivity $k = 0.1$ (data from Table 3). The run numbers 1–4 are defined with reference to a comprehensive set of heat flux distributions accommodated within equation (2) and given by

$$\begin{aligned} &1.\ q(x)/q = 1 \\ &2.\ q(x)/q = 1+0.2x-0.04x^2 \\ &3.\ q(x)/q = 1-0.2x+0.04x^2 \\ &4.\ q(x)/q = 1+0.2x. \end{aligned} \tag{31}$$

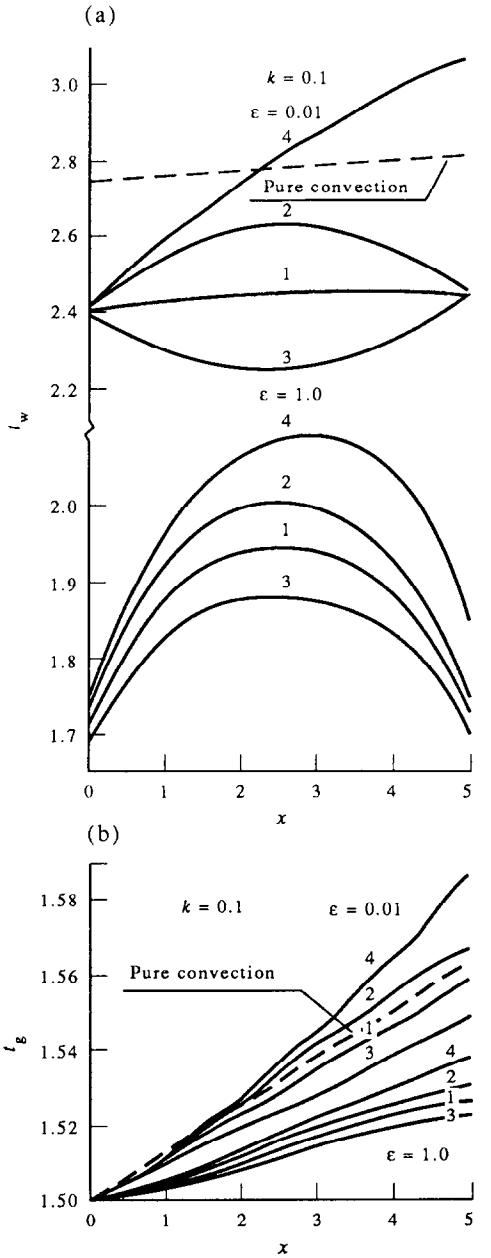

FIG. 4. (a) Effect of dimensionless (non-uniform) heat fluxes $q(x)/q$ on the tube wall temperature distribution. $k = 0.1$; $\varepsilon = 1.0$ and 0.01. (b) Effect of dimensionless (non-uniform) heat flux $q(x)/q$ on the gas temperature distribution. $k = 0.1$; $\varepsilon = 1.0$ and 0.01.

Table 3. Effect on predictions of varying dimensionless heat flux, for $\varepsilon = 1.0$ and 0.01 (heated tube)

$l = 5$ $H = 0.8$ $S = 0.01$ $t_{1,i} = t_{g,i} = 1.5$ $A = 0.85$ $k = 0.1$ $\varepsilon_p = 0.025$ $\varepsilon_{p,s} = 0.075$								
	$\varepsilon = 1.0$		$E = 1.1025$	$R = 3.12\times10^{-4}$		$\varepsilon = 0.01$	$E = 6.30$	$R = 1.0\times10^{-4}$
	1	2	3	4	1	2	3	4
$t_w(0) = t_{w,i}$	1.7065	1.7239	1.6889	1.7390	2.4085	2.4102	2.4070	2.4121
$t_{w,e} = t_w(l)$	1.7237	1.7431	1.7038	1.8484	2.4478	2.4556	2.4401	3.0750
$t_{r,e} = t_{g,e}$	1.5266	1.5305	1.5225	1.5372	1.5581	1.5673	1.5487	1.5854
Δb [%]	0.141	0.26	0.036	0.314	0.57	0.635	0.517	0.82

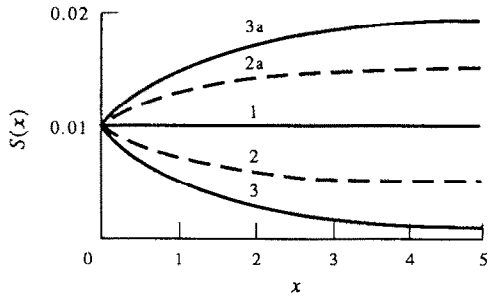

FIG. 5. Stanton number $S(x)$ distributions along the inner surface of the wall.

Effect of Stanton number

In a similar manner to heat flux, a set of alternative distributions for $h(x)$, accommodated by equation (3), result in the following run definitions for the dimensionless convective parameters $S(x)$ and $H(x)$:

$$\begin{aligned}
&1.\ S(x) = S = 0.01 \quad H(x) = H = 0.8\\
&2.\ S(x) = 0.01 - 0.0035x + 0.0005x^2\\
&\quad H(x) = 0.8 - 0.28x + 0.04x^2\\
&3.\ S(x) = 0.01 - 0.0058x + 0.0008x^2,\\
&\quad H(x) = 0.8 - 0.464x + 0.064x^2\\
&2a.\ S(x) = 0.01 + 0.0035x - 0.0005x^2\\
&\quad H(x) = 0.8 + 0.28x - 0.04x^2\\
&3a.\ S(x) = 0.01 + 0.0058x + 0.0008x^2\\
&\quad H(x) = 0.8 + 0.464x - 0.064x^2. \qquad (32)
\end{aligned}$$

Figure 5 illustrates the Stanton number $S(x)$ distributions along the inner surface of the wall. In Figs. 6 and 7 the results for different values of Stanton number $S(x)$ and of $H(x)$ are plotted for emissivities of 1 and 0.1 and dimensionless absorptivity $k = 0.0$ and 0.1. For the same uniform external heat flux, an increase in the Stanton number (examples $3 \rightarrow 3a$) tends to decrease the axial temperature distribution along the tube and increase the axial gas temperature gradient (Figs. 6(c) and 7(c)). The present results show that this parameter does not have a significant effect for $\varepsilon = 1.0$ but becomes quite large for an emissivity of 0.1. Also, it has a more conspicuous effect near the outlet reservoir. Tables 4 and 5 show the set of dimensionless numbers and physical quantities which were used in this calculation.

Results for cooled tubes

In refs. [1–3, 8, 10], and the previous section, the overall problem treated by various calculations and analyses for a flow system with transparent and radiation gas refers only to heated tubes. In this section of our paper, we extend the consideration to certain specific results for cooled tubes. These illustrate the influence of (i) the inlet and exit reservoir temperatures, (ii) the non-uniformity of a (negative) heat flux, (iii) the radiative properties of the radiation gas and

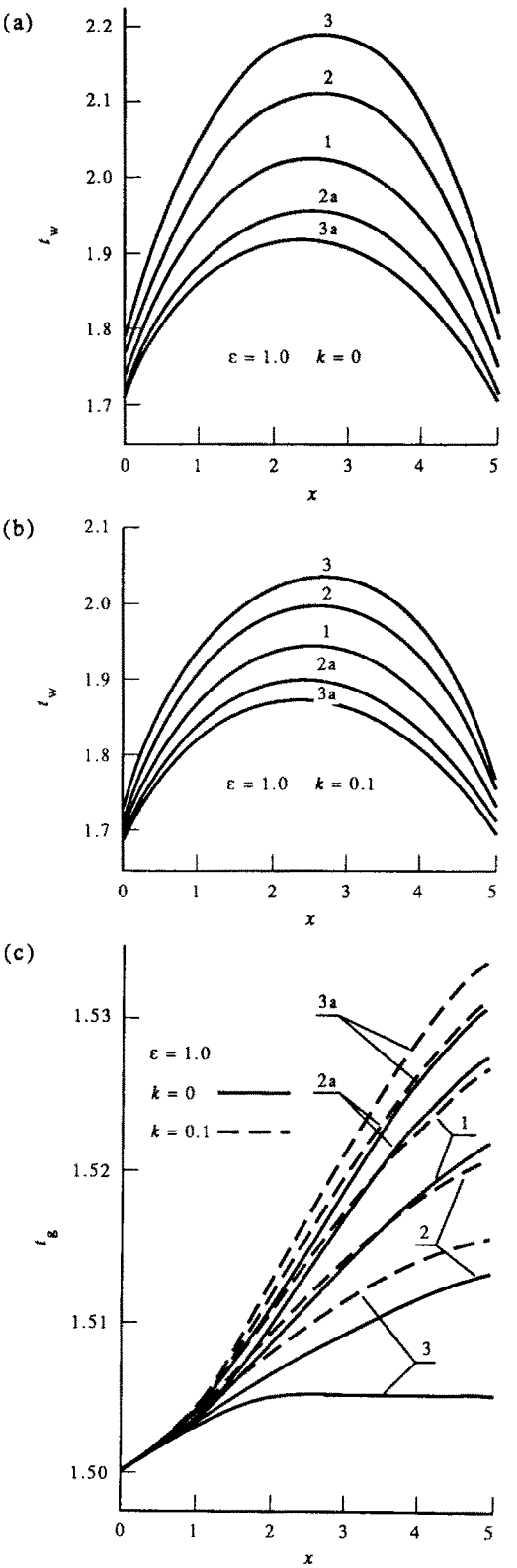

FIG. 6. (a) Effect of length-dependent Stanton number $S(x)$ on the temperature distributions in the tube wall. $k = 0.0$; $\varepsilon = 1.0$ (transparent gas). (b) Effect of length-dependent Stanton number $S(x)$ on the temperature distributions in the tube wall. $k = 0.1$; $\varepsilon = 1.0$ (radiation gas). (c) Effect of length-dependent Stanton number $S(x)$ on the temperature distributions in the gas. $k = 0.0$ and 0.1; $\varepsilon = 1.0$.

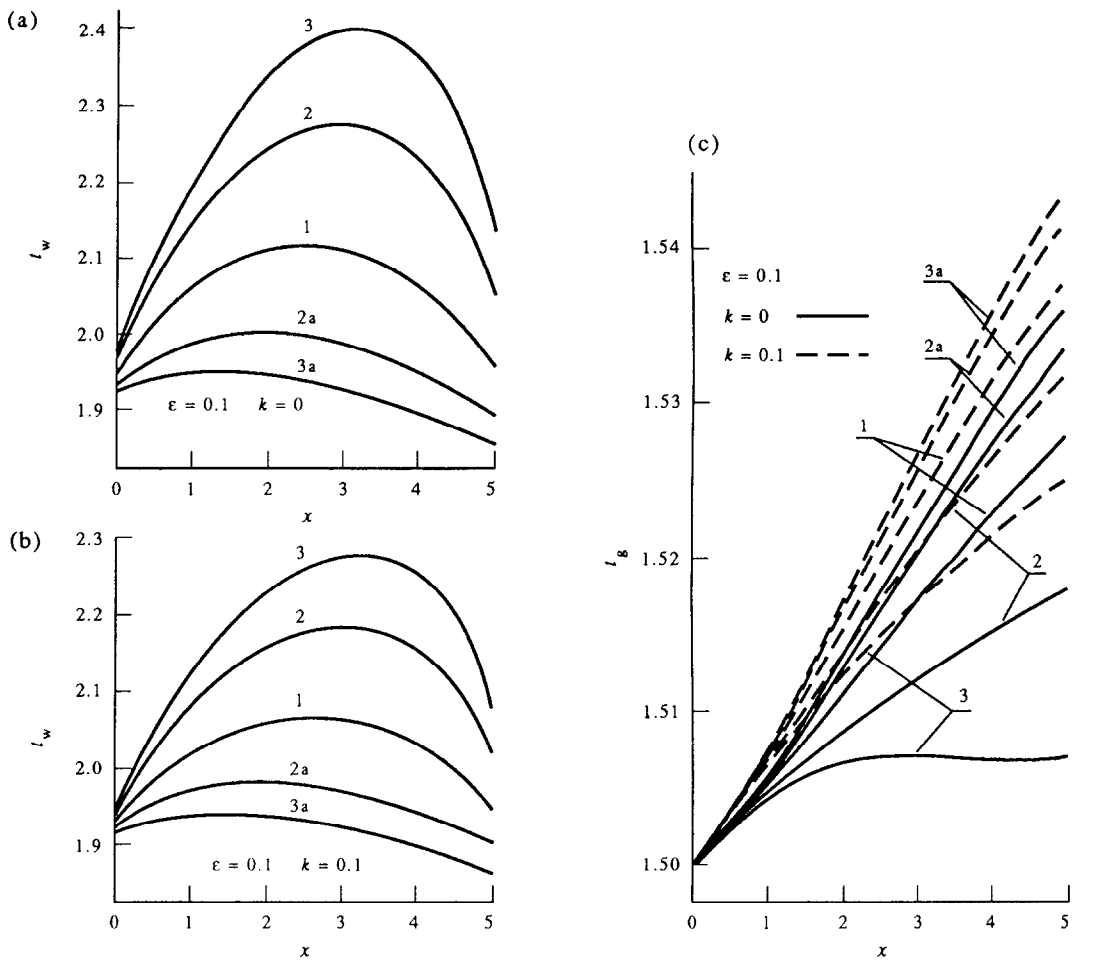

FIG. 7. (a) Effect of length-dependent Stanton number $S(x)$ on the temperature distributions in the tube wall. $k = 0.0$; $\varepsilon = 0.1$ (transparent gas). (b) Effect of length-dependent Stanton number $S(x)$ on the temperature distributions in the tube wall. $k = 0.1$; $\varepsilon = 0.1$ (radiation gas). (c) Effect of length-dependent Stanton number $S(x)$ on the temperature distributions in the gas. $k = 0.0$ and 0.1; $\varepsilon = 0.1$.

Table 4. Effect on predictions of length-dependent Stanton number, for $k = 0.0$ and 0.1 ($\varepsilon = 1.0$) (heated tube)

$l = 5 \quad H = 0.8 \quad S = 0.01 \quad t_{r,i} = t_{g,i} = 1.5 \quad A = 0.85$

	$\varepsilon = 1.0 \quad k = 0.0 \quad E = 1.0$ $\varepsilon_{p,s} = 0.0 \quad R = 0.0 \quad \varepsilon_p = 0.0$				$\varepsilon = 1.0 \quad k = 0.1 \quad E = 1.1025$ $\varepsilon_{p,s} = 0.075 \quad R = 3.12 \times 10^{-4} \quad \varepsilon_p = 0.025$			
	2	3	2a	3a	2	3	2a	3a
$t_w(0) = t_{w,i}$	1.7660	1.7890	1.7202	1.7095	1.7192	1.7295	1.6961	1.6901
$t_{w,e} = t_w(l)$	1.7917	1.8276	1.7236	1.7075	1.7462	1.7662	1.7059	1.6954
$t_{r,e} = t_{g,e}$	1.5132	1.5051	1.5274	1.5305	1.5207	1.5155	1.5310	1.5336
Δb [%]	0.01	0.113	0.05	0.074	0.21	0.284	0.09	0.058

Table 5. Effect on predictions of length-dependent Stanton number, for $k = 0.0$ and 0.1 ($\varepsilon = 1.0$) (heated tube)

$l = 5 \quad H = 0.8 \quad S = 0.01 \quad t_{r,i} = t_{g,i} = 1.5 \quad A = 0.85$

	$\varepsilon = 0.1 \quad k = 0.0 \quad E = 1.0$ $\varepsilon_{p,s} = 0.0 \quad R = 0.0 \quad \varepsilon_p = 0.0$				$\varepsilon = 0.1 \quad k = 0.1 \quad E = 1.575$ $\varepsilon_{p,s} = 0.075 \quad R = 3.12 \times 10^{-4} \quad \varepsilon_p = 0.025$			
	2	3	2a	3a	2	3	2a	3a
$t_w(0) = t_{w,i}$	1.9638	1.9775	1.9305	1.9225	1.9378	1.9433	1.9217	1.9169
$t_{w,e} = t_w(l)$	2.0516	2.1361	1.8969	1.8618	2.0221	2.0886	1.8973	1.8654
$t_{r,e} = t_{g,e}$	1.5177	1.5069	1.5331	1.5358	1.5314	1.5249	1.5411	1.5430
Δb [%]	0.348	0.51	0.248	0.335	0.382	0.41	0.137	0.095

Table 6. Input data and predicted exit temperatures for runs 1–3 (cooled tube)

$l = 5 \quad H = 8 \quad S = 0.01 \quad \varepsilon = 1.0 \quad k = 0.0$
$t_{g,i} = 2.0 \quad E = 1.0 \quad M = 0.0 \quad C = 0.0$

Run	$t_w(0) = t_{w,i}$				Δb [%]
1	1.8369	$t_{r,i} = t_{g,i} = 2.0$	$t_{r,e} = t_{w,e} = 0.776$	$t_{g,e} = 1.9606$	0.0
2	1.8388	$t_{r,i} = t_{g,i} = 2.0$	$t_{r,e} = 1.40$	$t_{g,e} = 1.9665$	0.0
			$t_{w,e} = 1.2535$		
3	1.6346	$t_{r,i} = 1.8$	$t_{r,e} = t_{w,e} = 0.736$	$t_{g,e} = 1.9539$	0.0
		$t_{g,i} = 2.0$			

(iv) the influence of tube length on the wall and gas temperature distribution. Tables 6–8 show the set of dimensionless numbers and physical quantities which are used in the calculation. The initial and final wall and radiation gas temperatures, all calculated numerically, are also presented there. Also, in Tables 6–8 is an expression of the accuracy of the method Δb[%].

Effect of inlet and exit reservoir temperatures

Figure 8 shows the effect of varying the inlet and exit reservoir temperature in a duct of length $x = 5$. Solutions were obtained for a transparent gas and uniform (negative) heat flux. For a fixed inlet gas temperature $t_{g,i} = 2.0$ the inlet reservoir temperature $t_{r,i}$ was set equal to $t_{g,i}$ (for runs 1 and 2) while for run 3 it was assumed to be 1.8. Also, for runs 1 and 3 the exit reservoir temperatures were set equal to the exit wall temperature ($t_{r,e} = t_{w,e}$). For run 2 it was assumed that the exit reservoir temperature $t_{r,e} = 1.40$ was a parameter independent of the exit gas and wall temperatures. As shown in Fig. 8 the initial portion of the wall-temperature curve is nearly independent of the exit reservoir temperature because the exit reservoir is too far away to influence the region near the tube inlet [1, 2].

Table 7. Input data and predicted exit temperatures for runs 4–7 (cooled tube)

$l = 5 \quad H = 0.8 \quad S = 0.01 \quad \varepsilon = 1.0$
$A = 1.18 \quad t_{g,i} = t_{r,i} = 2.0$

	$k = 0.0$ $R = 0.0$ $E = 1.0$ $\varepsilon_{p,s} = 0.0$	$k = 0.1$ $E = 1.1025$	$R = 3.125 \times 10^{-4}$ $\varepsilon_{p,s} = 0.075$	
Run	4	5	6	7
M	0.0	0.0	0.20	−0.20
C	0.0	0.0	−0.04	0.04
$t_w(0) = t_{w,i}$	1.8499	1.9201	1.9111	1.9293
$t_{w,e} = t_w(l)$	1.8284	1.9080	1.8935	1.9222
$t_{r,e} = t_{g,e}$	1.9794	1.9879	1.9837	1.9919
Δb [%]	0.0	1.78	1.93	1.64

Table 8. Input data and predicted exit temperatures for runs 8–11 (cooled tube)

$H = 0.8 \quad S = 0.01 \quad \varepsilon = 1.0 \quad A = 1.18$
$E = 1.21 \quad t_{g,i} = t_{r,i} = 1.5 \quad k = 0.2$
$\varepsilon_{p,s} = 0.15 \quad R = 6.25 \times 10^{-4}$

Run	8	9	10	11
	$l = 5$	$l = 8$	$l = 10$	$l = 16$
$t_w(0) = t_{w,i}$	1.3284	1.3275	1.3275	1.3275
$t_{w,e} = t_w(l)$	1.2936	1.2593	1.2359	1.1621
$t_{r,e} = t_{g,e}$	1.4727	1.4491	1.4328	1.3820
Δb [%]	1.65	2.62	3.25	5.11

Effect of (negative) heat flux

Figure 9 shows the wall and gas temperature distributions for short tubes with various (negative) heat fluxes and for $k = 0.0$ and 0.1. When the absorptivity of the radiation gas is increased, the radiation-heat transfer becomes more efficient and hence the wall

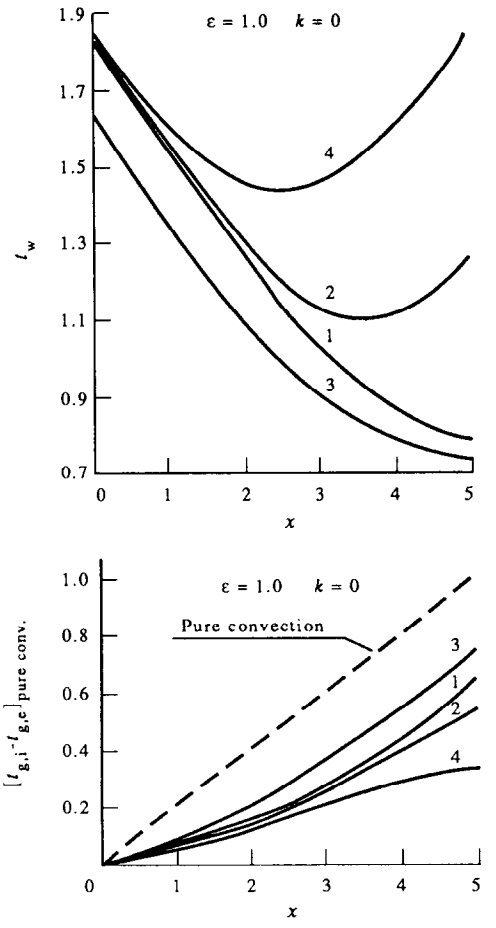

FIG. 8. Effect of inlet and exit reservoir temperature on the temperature distributions in the tube wall and gas. $\varepsilon = 1.0$; $k = 0.0$ (transparent gas).

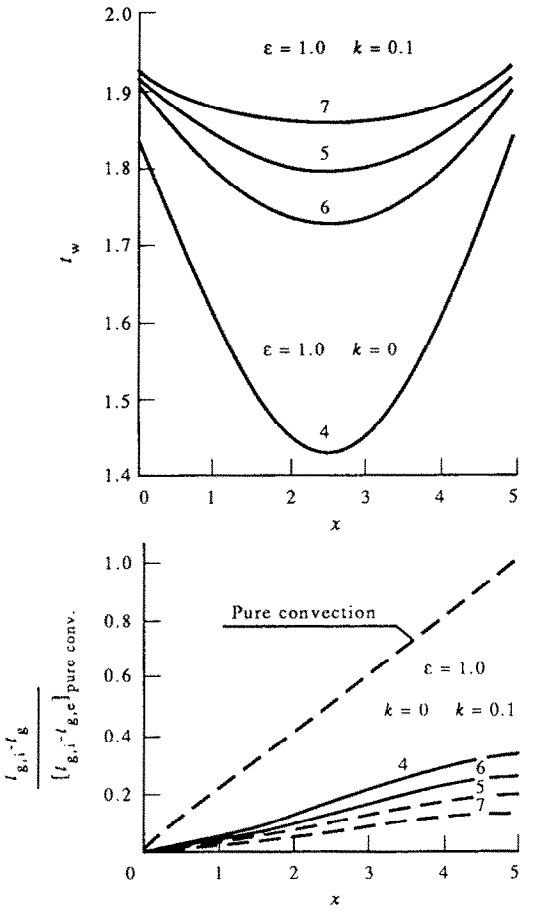

FIG. 9. Effect of dimensionless (non-uniform) heat fluxes on the temperature distributions in the tube wall and gas. $\varepsilon = 1.0$; $k = 0.0$ and 0.1.

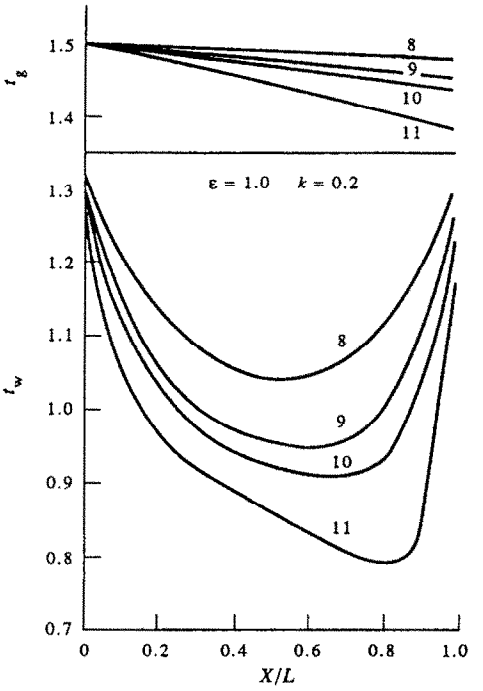

FIG. 10. Effect of tube length on the tube wall and gas temperature distributions. $q(x) = \text{const}$; $\varepsilon = 1.0$; $k = 0.2$.

temperature distributions increase. Because of the large radiation being transferred to the wall, the curves of radiation gas temperature fall far below the gas temperature for a transparent gas.

Effect of tube length–diameter ratio

The influence of dimensionless tube length l for a wall emissivity $\varepsilon = 1.0$ and dimensionless gas absorptivity $k = 0.2$ on wall tube and radiation gas temperature distributions is shown in Fig. 10. However, as l increases beyond about 16 diameters convergence becomes problematical due to the highly non-linear form of the equations. This displays itself in pseudo-solutions which are quite inconsistent with the downstream thermal boundary conditions used as a check during iteration. In fact, the above length itself appears to be dependent on temperature and dimensionless gas absorptivity k, and we have quoted the value relevant to Fig. 10.

CONCLUSIONS AND FUTURE WORK

In this paper we have presented a comprehensive treatment of the problem of combined radiation and convection for fluid flowing in a tube. In three important regards we have extended the analysis of Siegel and Perlmutter [1, 2]. However, we have retained both the general features of their approach, and for convenience of comparison, their notation.

Our analysis now includes (a) the effect of non-transparency of the gas, parameter k, (b) length-dependent heat fluxes, up to a parabolic distribution and (c) the application to cooled tubes.

Other features are an overall energy balance check (rarely above 1% error), and a flexible accommodation of convection. The latter means that either a dimensionless-group type expression, or even a CFD (computational fluid dynamics) approach could be used for the local convective heat transfer.

For the future, we also intend to study the effects of the various contributing factors to the overall energy balance, and to compare these with corresponding considerations in the other methods such as Monte-Carlo or heat flux. The convergence problem should also be investigated further.

REFERENCES

1. M. Perlmutter and R. Siegel, Heat transfer by combined forced and thermal radiation in a heated tube, *J. Heat Transfer* **84**, 301–311 (1962).
2. R. Siegel and M. Perlmutter, Convective and radiant heat transfer for flow of transparent gas in a tube with a gray wall, *Int. J. Heat Mass Transfer* **5**, 639–660 (1962).
3. J. Stasiek, Application of the generalised configuration factors and the principle of surface transformation to radiant heat exchange in system with optically active

medium, *Z.N.P.G. Mechanika* **49,** 1–116 (1985) (in Polish).
4. H. C. Hottel and E. S. Cohen, Radiant heat exchange in gas-filled enclosure : allowance for nonuniformity of gas temperature, *A.I.Ch.E. Jl* **4,** 3–14 (1958).
5. H. C. Hottel and A. F. Sarofim, The effect of gas flow patterns on radiative transfer in cylindrical furnaces, *J. Heat Transfer* **8,** 1153–1169 (1965).
6. R. Siegel and J. R. Howell, *Thermal Radiation Heat Transfer*. McGraw-Hill, New York (1972, 1981).
7. M. W. Collins and J. Stasiek, Numerical modelling of radiative and convective heat transfer for flows of a non-transparent gas in a tube with grey wall. *Adv. Computational Meths in Heat Transfer*. Vol. 1. *Proc. 1st Int. Conf.*, Portsmouth, U.K., pp. 141–156, 17–20 July (1990).
8. J. Stasiek, Transformational-zone method of calculation of complex heat exchange of optically active medium inside tube of diffuse grey surface, *Wärme- und Stoffübertragung* **22,** 129–139 (1988).
9. J. Stasiek, J. Mikielewicz and A. Jedruch, Heat transfer during flow of optically active medium inside tube of diffuse grey surface, *Proc. 1st World Conf. Exp. Heat Transfer, Fluid Mech. Thermodynamics*, Dubrovnik, Yugoslavia, pp. 397–404, 4–9 September (1988).
10. J. Stasiek and M. W. Collins, Radiant and convective heat transfer for flow of an optically active gas in a cooled tube with a grey wall, *Proc. 9th Int. Heat Transfer Conf.*, Jerusalem, Israel, Vol. 6, pp. 409–414, 19–24 August (1990).
11. H. C. Hottel and A. F. Sarofim, *Radiative Transfer*. McGraw-Hill, New York (1967).
12. M. N. Özisik, *Radiative Transfer and Interactions with Conduction and Convection*. Wiley, New York (1973).
13. M. Perlmutter and J. R. Howell, Radiant transfer through a gray gas between concentric cylinders using Monte-Carlo, *J. Heat Transfer* **86,** 169–179 (1964).
14. C. M. Usiskin and R. Siegel, Thermal radiation from a cylindrical enclosure with specified wall heat flux, *J. Heat Transfer* **82,** 369–374 (1960).
15. IBM Application Program, Tech. Publ. Dept., New York (1970).